https://doi.org/10.5194/egusphere-2026-4424
Preprint. Discussion started: 14 August 2026

Submicron volcanic ash detected in sulfate aerosol mixtures observed by the Atmospheric Chemistry Experiment satellite

Michael Lecours[1], Chris D. Boone[1], and Peter F. Bernath[2,1]

[1]Department of Chemistry, University of Waterloo, 200 University Ave. W, Waterloo, ON N2L 3G1, Canada
[2]Department of Chemistry & Biochemistry, Old Dominion University, 4541 Hampton Blvd., Norfolk, VA 23529, USA

Correspondence to: Michael Lecours (mlecours@scisat.ca)

Abstract. Mixtures of volcanic ash and stratospheric sulfate aerosol (SSA) have been observed by the Atmospheric Chemistry Experiment (ACE), a remote sensing satellite mission in operation since 2004. The migration of the volcanic plumes from the Puyehue-Cordón Caulle eruption in June of 2011 and the Calbuco eruption of April 2015 aligned well with ACE's sampling pattern, providing extended sampling of volcanic aerosol from these two eruptions. Weak volcanic ash spectral signatures are observed in the presence of SSA in the Southern Hemisphere up to 165 days following the Calbuco eruption and 125 days following the Puyehue-Cordón Caulle eruption. ACE residual spectra of ash-sulfate mixtures were simultaneously modelled to retrieve the line-of-sight column densities and the median particle radii for both ash and SSA. Pure volcanic ash from the Puyehue-Cordón Caulle eruption was modelled with a bimodal lognormal distribution.

1 Introduction

Explosive volcanic eruptions can inject large amounts sulfur dioxide (SO_2) and volcanic ash into the upper troposphere and lower stratosphere. Sulfur dioxide is converted through a series of reactions into sulfuric acid which then forms liquid aerosol comprised of mainly sulfuric acid and water (McCormick et al., 1995). It is well known that sulfuric acid aerosol, hereby referred to as stratospheric sulfate aerosol (SSA), are important for the Earth's climate system because they simultaneously scatter incoming solar radiation and absorb out-going thermal radiation; the net radiative effect typically cools the Earth's surface (Kremser et al., 2016; Lacis et al., 1992). In addition to climate effects, SSA affects atmospheric chemistry by depleting ozone (Hofmann and Solomon, 1989; Solomon, 1999), and SSA can act as seed particles for polar stratospheric clouds (Carslaw et al., 1997; Peter and Grooß, 2011) that form during polar night in the Arctic and Antarctic winters.

Volcanic ash is typically ignored in climate models following large volcanic eruptions because large, high density silicate particles sediment quickly (Niemeier et al., 2009). However, small ash particles have been observed to persist in the atmosphere for many months (Gangale et al., 2010; Griessbach et al., 2014; Vernier et al., 2016). Recent works have shown that small volcanic ash particles can influence stratospheric SO_2 lifetimes (Zhu et al., 2020) and cause diabatic self-lofting of the volcanic plume (Khaykin et al., 2022). The infrared spectral signature of volcanic ash is relatively simple with only a Si-O absorption

https://doi.org/10.5194/egusphere-2026-4424
Preprint. Discussion started: 14 August 2026

around 1100 cm^{-1}, which has been observed with both in situ measurements (Deshler et al., 1993; Vernier et al., 2016) and by remote sensing with satellites (Gangale et al., 2010; Griessbach et al., 2014; Lecours et al., 2022).

"Residual spectra" can be generated from infrared atmospheric spectra by dividing out known gas-phase contributions, yielding underlying spectra that primarily contain information on aerosol and clouds (Lecours et al., 2022). In a recent study, residual spectra from the Atmospheric Chemistry Experiment (ACE), a solar occultation remote sensing satellite mission launched in 2003 that continues to operate to this day, were analyzed to provide a global climatology of SSA particle size, H_2SO_4 weight percentage and line-of-sight column density throughout the ACE mission (Bernath et al., 2026). Only residual spectra that were clearly dominated by sulfate aerosol and could therefore be modelled well using sulfate aerosol optical constants were included in the data product. The study did not include results from sulfate aerosol mixed with other aerosols such as polar stratospheric clouds, ice or volcanic ash. In this paper, the spectra of SSA from Bernath et al. (2026) were analyzed for weak volcanic ash spectral signatures. It was found that ash-sulfate mixtures are observed occasionally throughout the entire mission. The satellite's sampling frequency is limited, up to 30 measurements per day, with a slow day-to-day variation in latitude. The migration of volcanic material from the Puyehue-Cordón Caulle (PCC) eruption on 4 June 2011 and the Calbuco eruption on 22 April 2015 aligned well with ACE's sampling pattern (Bernath, 2017), providing extended sampling of volcanic aerosol from these two eruptions. Ash-sulfate mixed volcanic aerosol from other large eruptions are present in ACE data but the sampling is limited.

2 Methods

The primary instrument on board ACE is a high-resolution Fourier transform spectrometer with a spectral range of 750 cm^{-1} to 4400 cm^{-1} and a spectral resolution of 0.02 cm^{-1}. The infrared spectra are processed on the ground to provide vertical profiles of atmospheric trace gas volume mixing ratios (VMRs). The current data processing version 5.3 retrieves vertical profiles for 46 trace gases (Boone et al., 2023). Following the retrieval of atmospheric trace gases, observed atmospheric spectra are divided by a calculated spectrum consisting of all known gas-phase contributions resulting in a "residual" spectrum that is primarily the underlying spectrum of clouds and/or aerosol (Lecours et al., 2022). The calculated spectrum employs VMR profiles from ACE v5.3 retrievals and spectroscopic constants from HITRAN2020 (Gordon et al., 2022).

A detailed description of the calculation and calibration of residual spectra dominated by sulfate aerosol is presented in Bernath et al. (2026) and only a brief description is provided here. There are systematic errors in ACE residual spectra resulting from missing lines in the HITRAN2020 line list, most notably from nitric acid (HNO_3). To minimize these errors, ACE residual spectra are calibrated by a nearby background measurement to cancel out remaining systematic features; details for calibration are outlined in Bernath et al. (2026). A standard Levenberg-Marquardt least squares optimization routine was employed using the sulfuric acid optical constants from Lund Myhre et al. (2003) to retrieve the optimal H_2SO_4 weight percentage, median radius (assuming log-normal particle distribution with spread S=1.6) and line-of-sight particle column density. For sulfate aerosol, the extinction spectrum below ~3700 cm^{-1} arises primarily from absorption, while extinction above ~3700 cm^{-1} is

https://doi.org/10.5194/egusphere-2026-4424
Preprint. Discussion started: 14 August 2026

primarily from scattering. A data point from the 1.02 µm imager was included in the analysis to help stabilize the retrieval of the median radius because the extinction signal at that wavelength (primarily from scattering) is typically more sensitive to aerosol size than the scattering signal between 3700 and 4400 cm^{-1} from the FTS. This approach was taken for all residual spectra in the ACE dataset between 10 and 28 km filtering out any fitted results that had large errors on the retrieved parameters and/or large chi squared fit values. In this study the unfiltered dataset (every residual spectrum for which the fitting converged) from Bernath et al. (2026) was simulated as an ash-sulfate mixture to identify spectra that contain weak ash signals. Residual spectra that do not contain ash fail to converge or result in an overall higher chi squared value, while spectra that do contain weak ash improve the overall chi square value of the least-squares fitting. This method was used to identify ash-sulfate mixtures throughout the mission. The method does not extensively search for all possible ash-sulfate in the ACE dataset but likely identifies the majority of cases. False positive ash-sulfate identifications were manually removed from the analysis. In total 772 occultations were found to contain ash-sulfate, spread throughout the mission with 262 occultations (399 spectra) immediately following the PCC eruption and 192 occultations (667 spectra) following the Calbuco eruption. The volcanic material from the Calbuco eruption reached higher altitudes allowing more spectra per occultation to be recorded.

The transmission spectrum of volcanic ash and sulfate aerosol mixtures were modelled using the Beer-Lambert equation shown below.

$$T = A\exp(-\alpha_{sul}\cdot L_{sul} - \alpha_{ash}\cdot L_{ash}) \quad (1)$$

In this representation it is assumed that the two particles are non-interacting, such that the total aerosol extinction along the line of sight is the sum of individual extinctions. Separate extinction coefficients (α) in units of inverse distance and path lengths (L) in units of distance are needed to model combined transmission spectrum. The extinction coefficients are calculated by integrating the particle distribution, $n(r)$ with the extinction cross section σ_{ext}.

$$\alpha = \int_0^\infty dr\, n(r)\sigma_{ext} \quad (2)$$

Assuming spherical particles, extinction cross sections were calculated using miepython (Prahl, 2026) employing the optical constants from Lund Myhre et al. (2003) for the sulfuric acid contribution and the optical constants from Deguine et al. (2020) for the volcanic ash contribution. A monomodal lognormal particle distribution was assumed for each aerosol with N_0 representing the particle density (particles per cm^3). S is the spread of the distribution (often referred to as the geometric width) and r_m is the median radius.

$$n(r) = \frac{N_0}{\sqrt{2\pi}}\frac{1}{r}\frac{1}{\ln S}\exp\left(-\frac{(\ln r - \ln r_m)^2}{2(\ln S)^2}\right) \quad (3)$$

https://doi.org/10.5194/egusphere-2026-4424
Preprint. Discussion started: 14 August 2026

Assuming a constant particle density (N_0) and factoring it out from the integral, the extinction coefficient α can be rewritten in terms of the extinction cross section averaged over the particle distribution, C_{ext} in units of distance^2 / particle.

$$\alpha = N_o \cdot C_{ext} \tag{4}$$

This representation is useful for ACE measurements because it is not possible for ACE to separate the path length (L) from the particle density (N_0) because the signal from a small, dense plume will look identical to that from a large, diffuse plume along the line of sight. For this reason, the line-of-sight column density ($N_l = N_0 \cdot L$) in particles/cm^2 is introduced into equation 1.

$$T = A \exp(-N_l^{sul} \cdot C_{ext}^{sul} - N_l^{ash} \cdot C_{ext}^{ash}) \tag{5}$$

The parameter A is a baseline scaling parameter, usually close to 1.0; it is introduced to account for small errors that can arise in the calibration of the atmospheric spectrum. Separate baseline parameters are determined for the two FTS detectors: the mercury cadmium telluride (MCT) detector operating from 750 to 1835 cm^{-1} and the indium antimonide (InSb) detector operating from 1835 to 4400 cm^{-1}. Note that A = 1.0 for the imager data point because it is not possible to determine a baseline from a single point. Using separate baseline scaling for the FTS data and the imager data point introduces an (unavoidable) additional layer of uncertainty.

The integral over the particle distribution was evaluated using a Gauss-Legendre quadrature with enough quadrature points such that averaged extinction cross sections (C_{ext}) converged to 10^{-5}. Look up tables of averaged extinction cross sections were precalculated on an evenly spaced grid from r_m = 0.02 to 2.0 µm in steps of 0.02 µm and S = 1.1 to 1.6 in steps of 0.1. A standard Levenberg-Marquardt least squares minimization routine was used to retrieve the optimal column densities and median radii for a mixture of ash and sulfate aerosol particles. The ash-sulfate mixtures employed a fixed value of S = 1.6 for both aerosol types while pure volcanic ash optimizations utilized the full range of S values.

The optical constants for sulfuric acid are functions of temperature and H_2SO_4 weight percentage and the particles are assumed to be spherical. The infrared spectrum of ash is relatively simple with only one major Si-O absorption around 1100 cm^{-1} that shoulders the major sulfate feature at 1200 cm^{-1}, but it does not overlap with the major H_2O features around 3200 cm^{-1}, minimally impacting the sensitivity of the H_2SO_4 weight percentage retrieval (see Figure 1). To minimize the number of retrieved parameters and complexity of the least squares, the temperature was fixed to ACE v5.3 tangent temperature and the H_2SO_4 weight percentage was fixed to optimal weight percentage from Bernath et al. (2026). The ash optical constants are dependent on the source volcano and ash particles are not necessarily spherical. It would be more appropriate to model the mixed ash particles as non-spherical scatterers using the T-matrix method from Mishchenko and Travis (1998) along with a bimodal distribution. However, the ash contribution to these mixed spectra is relatively weak and only weakly sensitive to the axial ratio (see Figure S1), leading to ill conditioned least squares optimization when the axial ratio is included in the least

https://doi.org/10.5194/egusphere-2026-4424
Preprint. Discussion started: 14 August 2026

squares routine. The fitting used an uncertainty of 0.01 for most FTS data points, which was decreased for the imager point (0.001) and FTS data in the spectral range 950 -1300 cm^{-1} (0.005), the key diagnostic spectral region for both ash and sulfate in the infrared. Although not representative of the actual relative uncertainties in the data, the weightings resulting from these assumed uncertainties improved convergence for the least squares minimization.

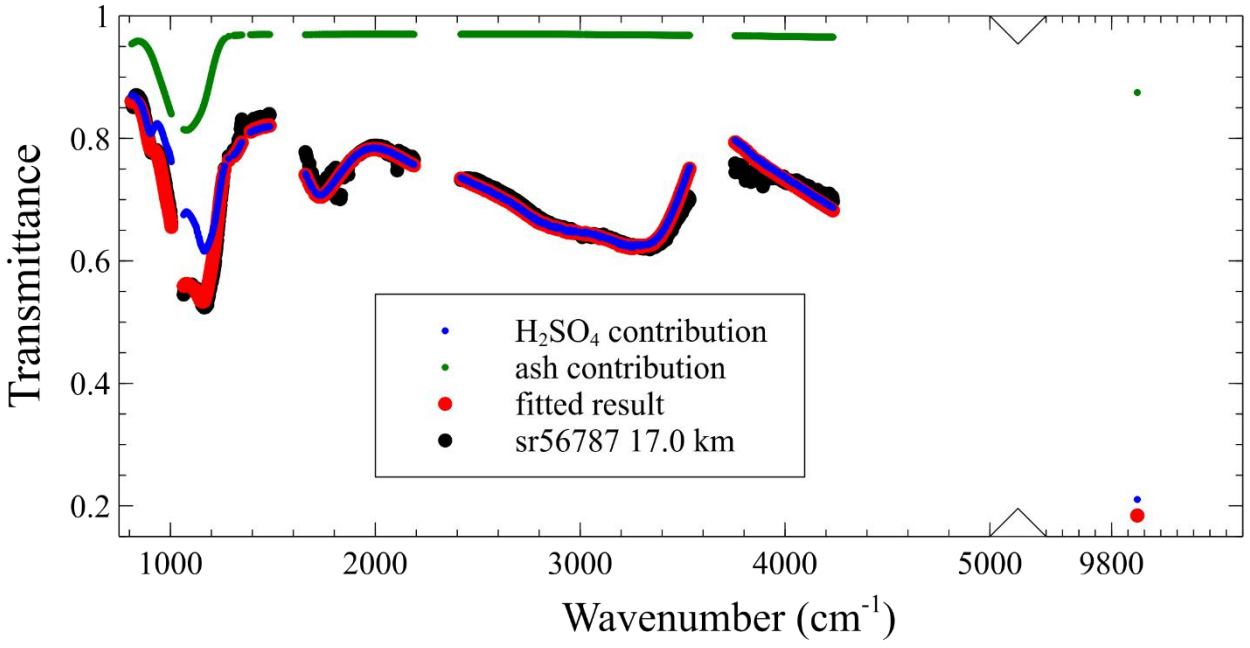

Figure 1: Residual spectrum for sr56787 at tangent height 17.0 km (black), recorded on 27 February 2014 following the Kelud eruption 14 days earlier. The optimized ash-sulfate mixture fitted result is shown in red along with the individual sulfate (blue) and ash (green) contributions.

Figure 1 depicts the residual spectrum from sr56787 at tangent height 17.0 km recorded on 27 February 2014 at latitude 7.09 °S and longitude 118.41 °E. The ACE occultation naming convention is sr (sunrise) or ss (sunset) followed by the satellite orbit number. This occultation was recorded 14 days after the Kelud eruption 13 February 2014 at 7.55 °S and 112.18 °E. The red dots in Figure 1 represent the overall ash-sulfate fitted results while blue dots represent the sulfate contribution and the green dots represent the ash contribution; note the imager point is included at 9803.92 cm^{-1}. The retrieved parameters for the ash contributions were N_l = 2.41 x 10^9 ± 1.4 x 10^8 particles/cm^2 and r_m = 0.058 ± 0.001 µm, and the sulfate contributions were N_l = 1.21 x 10^8 ± 2.6 x 10^6 particles/cm^2 and r_m = 0.326 ± 0.003 µm. The fitted spectrum in Figure 1 models the combination ash and sulfate absorptions reasonably well below 3500 cm^{-1} and slightly worse above 3500 cm^{-1} except for the heavily weighted imager point. A more appropriate analysis would be to model the sulfate contribution as a bimodal distribution, which is typical following a volcanic eruption (Deshler et al., 1993). In this retrieval, it is likely that the sulfate median radius is overestimated while the ash medium radius is underestimated.

https://doi.org/10.5194/egusphere-2026-4424
Preprint. Discussion started: 14 August 2026

To summarize the analysis, there are six retrieved parameters: MCT baseline scaling, InSb baseline scaling, ash line-of-sight column density (N_l^{ash}), sulfate line-of-sight column density ($N_l^{sulfate}$), ash median radius and sulfate median radius. The spread of the log-normal distributions was fixed to S = 1.6 for both ash and sulfate, and the temperature and H_2SO_4 weight percentage were fixed to the results of Bernath et al. (2026). The initial guess for the sulfate median radius was 90% of the sulfate aerosol median radius from Bernath et al. (2026) and the initial guess for ash was 0.1 μm. Residual spectra containing ash and polar stratospheric clouds, most notably nitric acid trihydrate (NAT), were removed from the analysis; see Figure S2 for an example of an ash-NAT mixture.

3 Results

ACE sampling frequency and geographic coverage are limiting factors in measuring volcanic ash following large eruptions. Ash can persist for many months in the atmosphere, and it can spread globally in a matter of days if the eruption injects material into the stratosphere. Ash from the PCC eruption was detected south of Australia in the days following the eruption (Klüser et al., 2013). ACE must be measuring in the correct location and correct time to detect ash. It is also difficult to assign the source of volcanic ash throughout the mission without a reasonably continuous dataset. For this reason, only the PCC and Calbuco eruptions are discussed.

Figure 2 depicts the locations of ACE measurements at 30 km tangent height from 5 to 11 June 2011. The data points are coloured based on days since 4 June 2011 when PCC violently erupted. The blue dots are the locations where ACE first detects residual spectra containing volcanic ash on 9 June 2011. On the day of the eruption, ACE was measuring at latitudes south of PCC complex and the sampling was migrating north. On 12 June 2011, the satellite entered a “high beta” gap where the angle between the satellite’s orbital track and the look-direction to the Sun is too large to record occultations (for ~2 weeks, the Sun never rises or sets for the orbiting satellite). Following the data gap, relatively pure ash was still observable along with ash-NAT and ash-sulfate mixtures that were recorded at all longitudes. It is not possible to tell if these mixtures are external (separate particles along the same line of sight) or internal (single hybrid particle).

https://doi.org/10.5194/egusphere-2026-4424
Preprint. Discussion started: 14 August 2026

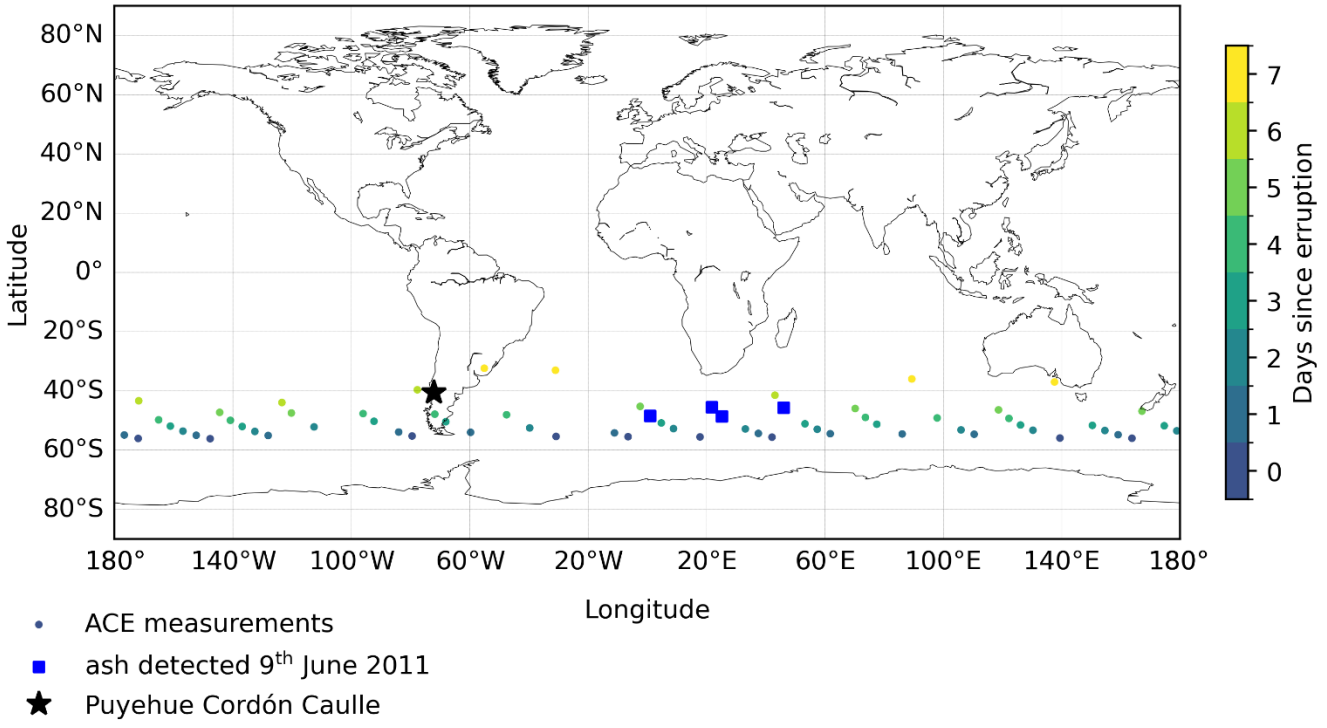

Figure 2: Location of ACE occultations from 5 June 2011 to 11 June 2011 coloured by days since the PCC eruption on 4 June 2011. The occultation in blue highlight where volcanic ash was detected.

Figure S3 panels a) and b) depict the locations of all ash-containing occultations from the PCC eruption and Calbuco eruptions, respectively. The ash observations migrate south from PCC for 125 days following the eruption. Observations end at 125 days because ACE measurements move north and do not return to the high southern latitudes until late November, at which time ash is no longer detected in ACE spectra. The Calbuco eruption yielded a similar longevity for ash-containing particles, with ash observed up to 165 days post eruption.

A pure ash spectrum from sr42562 at 10.5 km tangent height recorded on 7 July 2011 at 57.64 °S and 30.91 °W and calibrated by sr4850 at 11.3 km from the PCC eruption is depicted in Figure 3. A monomodal lognormal distribution was found to be insufficient to accurately model the ash absorption feature in this spectrum. Instead, a bimodal lognormal distribution (fine and coarse mode) was employed to more accurately model the infrared extinction. The spread (S) of the coarse and fine mode distributions were fixed while the median radius and line-of-sight column densities were retrieved. Every combination from S=1.1 to S=1.6 for both coarse and fine modes was attempted, and the lowest chi squared value occurred when S was fixed to 1.4 for both modes. The retrieved parameters for the coarse mode were N_l = 7.49 x 10^6 ± 4.5 x 10^5 particles/cm^2 and r_m = 0.740 ± 0.012 µm, and parameters for the fine mode were N_l = 1.89 x 10^9 ± 1.2 x 10^8 particles/cm^2 and r_m = 0.153 ± 0.003 µm.

https://doi.org/10.5194/egusphere-2026-4424
Preprint. Discussion started: 14 August 2026

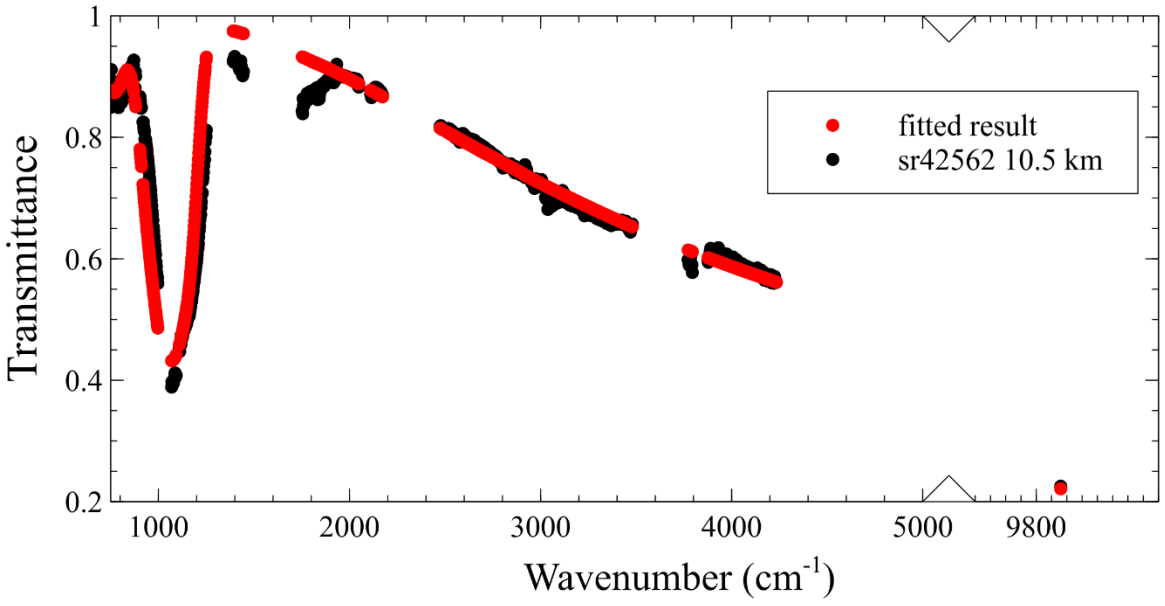

Figure 3: In black is a pure ash spectrum from sr42562 at 10.5 km tangent height recorded on 7 July 2011 at 57.64 °S and 30.91 °W, calibrated by sr4850 at 11.3 km. In red is the fitted bimodal ash spectrum.

The retrieved values from Figure 3 suggest the presence of at least two particle distributions below 1 µm. Previously, Bignami et al., (2014) estimated the effective radius of the PCC ash particles to be 4 to 5 µm, which would have a significantly different infrared spectrum: see Figure S1 compared to what is observed in Figure 3. The width of the absorption feature is sensitive to particle size due to the stronger scattering of bigger particles (Maes et al., 2016).

https://doi.org/10.5194/egusphere-2026-4424
Preprint. Discussion started: 14 August 2026

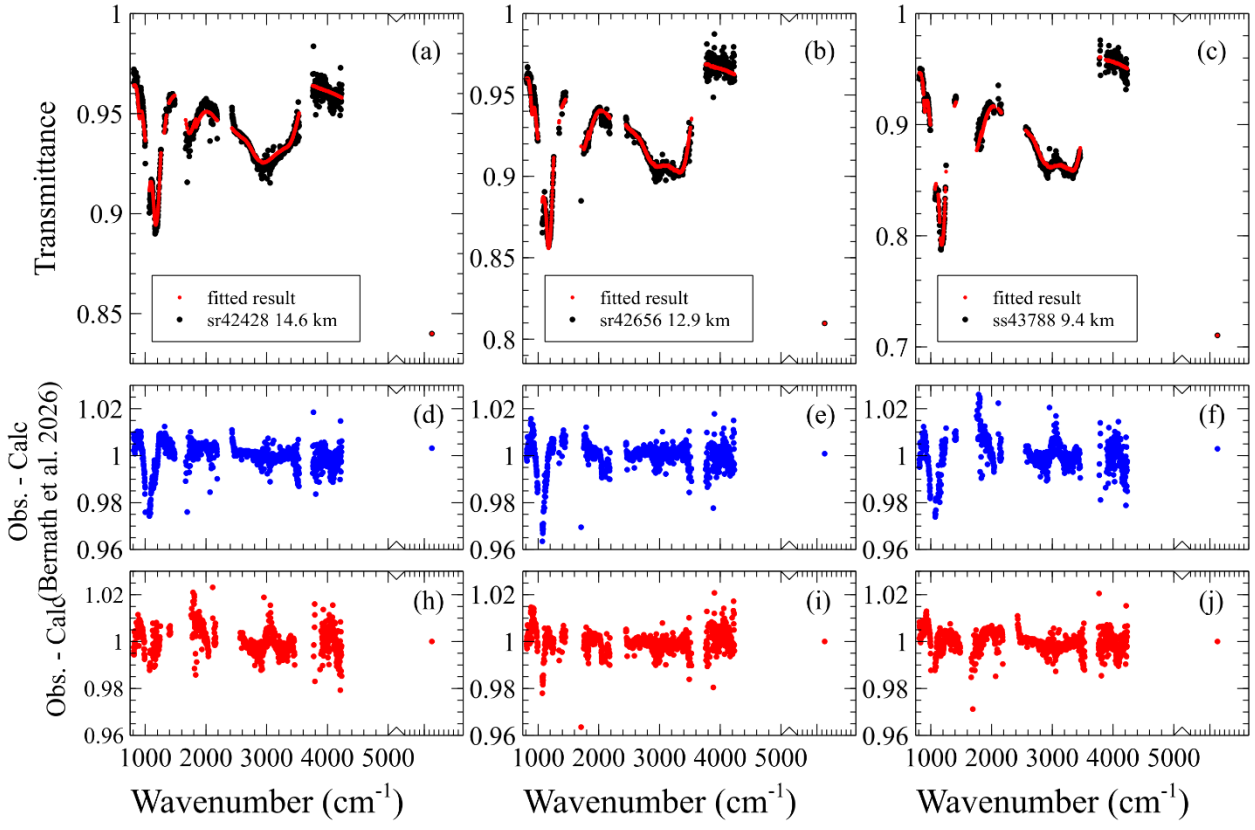

Figure 4: Each column represents data from a residual spectrum containing both ash and sulfate aerosol following the PCC eruption. For the top row (panels a, b, and c), measured residual spectra are shown in black, and mixed aerosol (ash+sulfate) fitting results are shown in red. a) sr42428 at 14.6 km recorded on 30 June 2011 at 35.15 °S and 20.24 °W. b) sr42656 at 12.9 km recorded on 15 July 2011 at 61.32 °S and 160.85 °W. c) ss43788 at 9.4 km recorded on 30 September 2011 at 58.42 °S and 50.99 °E. The middle row panels d, e and f represent the observed minus calculated residuals from sulfate aerosol only fitting results from Bernath et. al. (2026) where the residual ash signature is clearly visible. Panels h), i), and j) depict the observed minus calculated residuals from this work where the fitting assumes an ash-sulfate mixture.

Figure 4 depicts three residual spectra (panels 4a-4c) from three selected occultations sr42428 at 14.6 km recorded on 30 June 2011 at 35.15 °S and 20.24 °W (26 days after the PCC eruption), sr42656 at 12.9 km recorded on 15 July 2011 at 61.32 °S and 160.85 °W (41 days after the PCC eruption) and ss43788 at 9.4 km recorded on 30 September 2011 at 58.42 °S and 50.99 °E (118 days after the PCC eruption). The red dots in panels 4a-4c are the fitted ash-sulfate spectra and the black dots are the measured spectra. Panels 4d-4f depict the observed minus calculated sulfate only spectrum from the unfiltered fitted results in Bernath et al. (2026). In these residuals, the ash spectral feature near 1100 cm^{-1} is clearly visible, but the contribution to the overall spectrum is weak. The residual spectrum sr42428 14.6 km (panel 4a) was determined to be a mixed sulfate aerosol in Bernath et al. (2026) because the chi squared value was larger than the chosen threshold, and it was therefore excluded from the "pure sulfate" dataset. Higher altitude measurements above the ash layer in ss42428 are included in the Bernath et al.

https://doi.org/10.5194/egusphere-2026-4424
Preprint. Discussion started: 14 August 2026

(2026) dataset. The measurements in panels 4b and 4c were found to have small enough chi squared values for the least-squares fitting described in Bernath et al. (2026) that they were originally classified as pure sulfate aerosol.

The retrieved ash median radii for the three spectra shown in Figure 4 are similar in magnitude: 0.088 ± 0.016 µm, 0.081 ± 0.017 µm and 0.084 ± 0.023 µm for sr42428, sr42656 and ss43788, respectively, suggesting ash particle size remained relatively unchanged in the months following the PCC eruption. For these three spectra, the retrieved values for line-of-sight column density are $2.1x10^8 \pm 1.2x10^8$ particles/cm^2, $3.1x10^8 \pm 1.7x10^8$ particles/cm^2 and $2.5x10^8 \pm 1.9x10^8$ particles/cm^2, respectively. Percentage errors are smaller on median radius than on column density because the width of the ash absorption feature provides a relatively strong constraint on particle size.

Overall, the ash line-of-sight column density tends to decrease over time relative to the sulfate aerosol column density, as is shown in Figure 5 panel a) for measurements following the PCC eruption and in panel b) for the Calbuco eruption. The log column density ratios are coloured by 2 km altitude bins. For the Calbuco eruption, higher altitude (>14 km) ash-sulfate detections persist until 125 days post eruption. Below 14 km, ash-sulfate mixtures are detected up to 165 days. The aerosol from the PCC eruption follow a similar trend in which there is a steady decline in the ash-sulfate column density ratio over time.

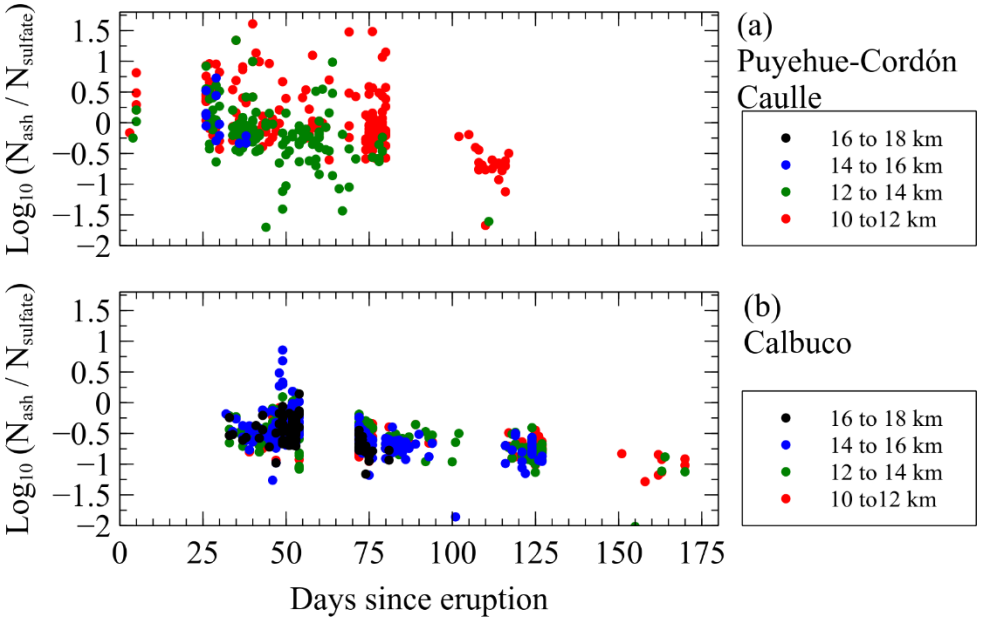

Figure 5: The ash-sulfate tangent column density ratio for measurements following the PCC eruption (panel a) and the Calbuco eruption (panel b). Measurements are coloured by altitude.

Figure 6 displays the sulfate median radius for pure SSA (black) from Bernath et al. (2026) and mixed ash-sulfates in red for the period following the PCC eruption (panel a) and the Calbuco eruption (panel b). In the first 100 days following the eruption,

https://doi.org/10.5194/egusphere-2026-4424
Preprint. Discussion started: 14 August 2026

the sulfate median radius is typically larger than the ash-free sulfates. After 100 days the ash-sulfate mixture becomes relatively indistinguishable in particle size from ash-free sulfate aerosol. The most reliable method to detect the presence of ash in long lived volcanic aerosol is by the infrared absorption and not by the sulfate aerosol particle size. The sulfate contribution for PCC ash-sulfate particles is typically larger than for Calbuco ash-sulfates. Close to the eruption there is a more significant difference in sulfate radius between the "pure sulfate" Bernath et al. (2026) particles and the ash-sulfate particles. Similarly to the Calbuco eruption around 90 days the PCC ash-sulfate aerosol are essentially the same size as the particles in Bernath et al. (2026).

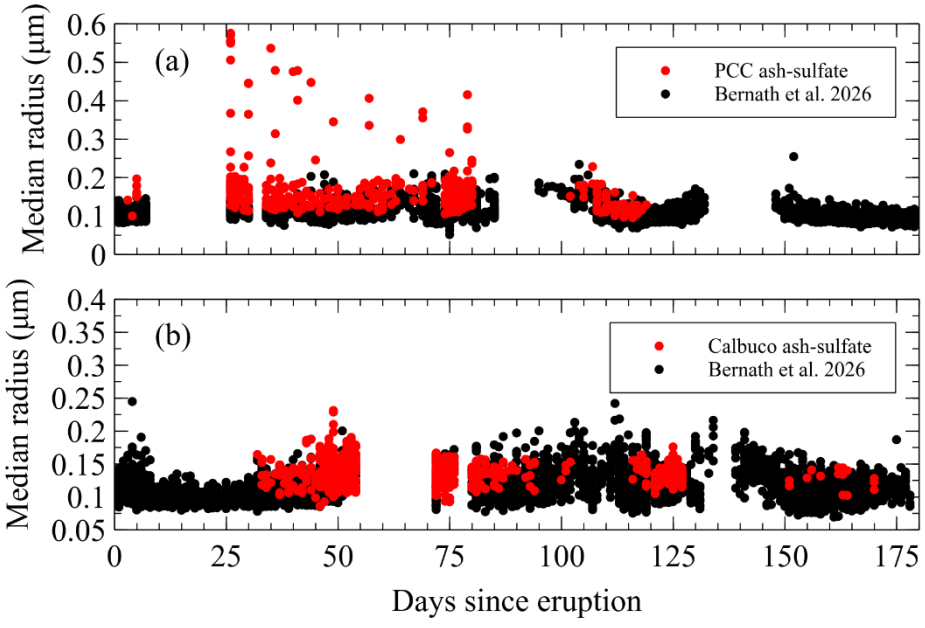

Figure 6: Sulfate median radius for the ash-sulfate mixed aerosol (red) and without ash (black) following the PCC eruption (panel a) and the Calbuco eruption (panel b).

The median radius for the ash contribution is relatively consistent in all detections ranging between 0.05 μm and 0.1 μm. The retrieved median radius from the PCC eruption is shown in Figure 7 panel a) and panel b) for the Calbuco eruption. The average ash median radius from the Calbuco eruption was found to be 0.087 μm while ash median radius for the PCC eruption was found to be 0.088 μm on average.

https://doi.org/10.5194/egusphere-2026-4424
Preprint. Discussion started: 14 August 2026

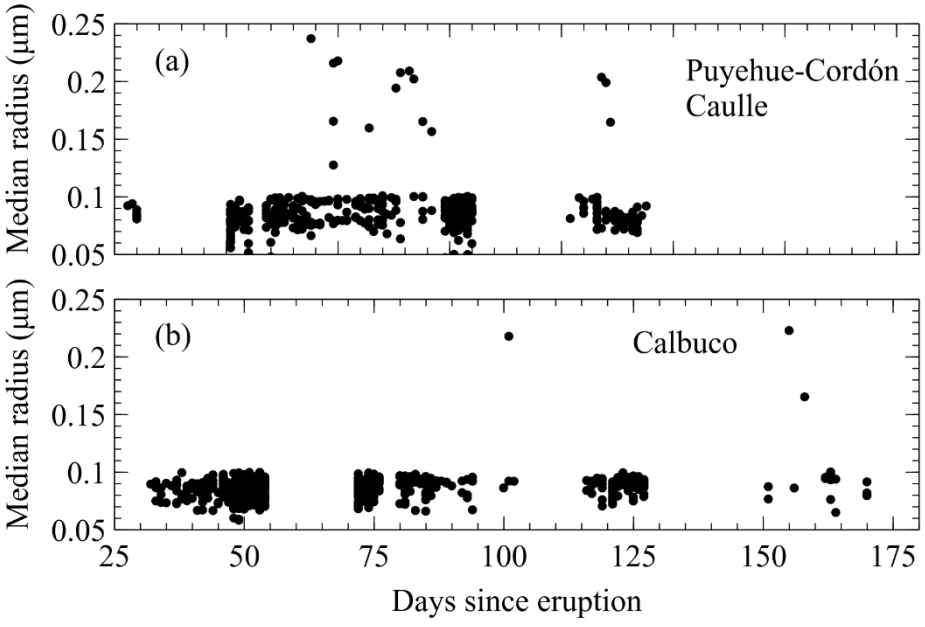

Figure 7: Median radius for the ash contribution following the PCC eruption (panel a) and the Calbuco eruption panel b).

4 Conclusions

Submicron ash particles have been detected in the presence of stratospheric sulfate aerosol throughout the ACE dataset. Fitted results suggest the presence of at least two submicron distributions of volcanic ash following the Puyehue-Cordón Caulle eruption. An extremely fine mode of ash particles can persist in the presence of stratospheric sulfate aerosol for many months following a stratospheric injection. The median radius for sulfate aerosol that contain weak ash is relatively unchanged from ash-free results reported in Bernath et al. (2026) and should have minimal impact on that data product.

A distinctive Si-O spectral feature in silicate ash permits the identification of volcanic ash particles in atmospheric infrared spectra from the ACE satellite mission. The contribution to the atmospheric spectrum from ash is often weak and typically requires a simultaneous fitting of the contribution from sulfate aerosol (another common byproduct of volcanic eruptions) to permit a quantitative analysis. There is no way to tell from the infrared spectrum whether the mixture of sulfate and ash contributions is associated with separate particles along the line of sight or indicates hybrid particles.

Observing extreme fine mode (median radius < 0.1 μm) ash particles in the stratosphere following a strong volcanic eruption is a relatively common occurrence. These fine mode particles can persist for several months after injection. In the Southern Hemisphere, two separate eruptions aligned well with ACE sampling, allowing ash to be tracked over an extended period. Ash was observed in ACE spectra for 125 days following the Puyehue-Cordón Caulle eruption in 2011 and 165 days following the

https://doi.org/10.5194/egusphere-2026-4424
Preprint. Discussion started: 14 August 2026

Calbuco eruption in 2015. Ash particles may have persisted longer than that for these eruptions, but ACE measurements moved out of the affected region and could no longer track them.

Nearly pure ash measurements from the Puyehue-Cordón Caulle eruption required at least two size distribution modes to accurately reproduce the observations. Both modes from a bimodal fit to the data had a submicron median radius. No instances of ash with median radius greater than 1 μm were observed in the ACE data, but that could be due to the sparse sampling offered by solar occultation and the fact that large ash particles would quickly settle out of the atmosphere.

Some measurements that were designated "pure sulfate" from the Bernath et al. (2026) study contained weak ash contributions, sufficiently weak for the measurements to pass through the "fit quality" filter applied to the dataset. Simultaneously analysing sulfate and ash contributions to the measurements yielded minimal change to the sulfate parameters (weight percent H_2SO_4 and median radius), suggesting that ignoring weak ash contributions should have little impact on the data quality in the Bernath et al. (2026) dataset.

Data availability

ACE-FTS volume mixing ratio and imager retrievals can be accessed at https://databace.scisat.ca/level2/ace_v5.3/display_data.php (registration required). The ash-sulfate aerosol data used in the study are available at Zenodo via https://doi.org/10.5281/zenodo.21479502

Supplement link

The link to the supplement will be included by Copernicus, if applicable.

Author contributions

M. Lecours developed the software, performed the analysis and prepared the manuscript. C. Boone assisted with the analysis and software in addition to reviewing and editing of the manuscript. P. Bernath provided supervision and reviewing and editing of the manuscript.

Competing interests

Authors declare no conflicts of interest.

https://doi.org/10.5194/egusphere-2026-4424
Preprint. Discussion started: 14 August 2026

Acknowledgements

Funding is provided by the Canadian Space Agency (9F045-230421/001), Funding was also provided by the National Aeronautics and Space Administration grant 80NSSC23K0999. PB acknowledges RB for productive discussion.

Review statement

The review statement will be added by Copernicus Publications listing the handling editor as well as all contributing referees according to their status anonymous or identified.

References

Bernath, P., Bhusal, M., Lecours, M., and Boone, C.: Global Characterization of Stratospheric Sulfate Aerosols by the Atmospheric Chemistry Experiment (ACE), J. Geophys. Res. Atmos., 131, e2025JD046214, https://doi.org/https://doi.org/10.1029/2025JD046214, 2026.

Bernath, P. F.: The Atmospheric Chemistry Experiment (ACE), J. Quant. Spectrosc. Radiat. Transf., 186, 3–16, https://doi.org/10.1016/j.jqsrt.2016.04.006, 2017.

Bignami, C., Corradini, S., Merucci, L., de Michele, M., Raucoules, D., De Astis, G., Stramondo, S., and Piedra, J.: Multisensor Satellite Monitoring of the 2011 Puyehue-Cordon Caulle Eruption, IEEE J. Sel. Top. Appl. Earth Obs. Remote Sens., 7, 2786–2796, https://doi.org/10.1109/JSTARS.2014.2320638, 2014.

Boone, C. D., Bernath, P. F., and Lecours, M.: Version 5 retrievals for ACE-FTS and ACE-imagers, J. Quant. Spectrosc. Radiat. Transf., 310, 108749, https://doi.org/10.1016/j.jqsrt.2023.108749, 2023.

Carslaw, K. S., Peter, T., and Clegg, S. L.: Modeling the composition of liquid stratospheric aerosols, Rev. Geophys., 35, 125–154, https://doi.org/10.1029/97RG00078, 1997.

Deguine, A., Petitprez, D., Clarisse, L., Guðmundsson, S., Outes, V., Villarosa, G., and Herbin, H.: Complex refractive index of volcanic ash aerosol in the infrared, visible, and ultraviolet, Appl. Opt., 59, 884–895, https://doi.org/10.1364/AO.59.000884, 2020.

Deshler, T., Johnson, B. J., and Rozier, W. R.: Balloonborne measurements of Pinatubo aerosol during 1991 and 1992 at 41°N: Vertical profiles, size distribution, and volatility, Geophys. Res. Lett., 20, 1435–1438, https://doi.org/10.1029/93GL01337, 1993.

Gangale, G., Prata, A. J., and Clarisse, L.: The infrared spectral signature of volcanic ash determined from high-spectral resolution satellite measurements, Remote Sens. Environ., 114, 414–425, https://doi.org/10.1016/j.rse.2009.09.007, 2010.

Gordon, I. E., Rothman, L. S., Hargreaves, R. J., Hashemi, R., Karlovets, E. V., Skinner, F. M., Conway, E. K., Hill, C., Kochanov, R. V., Tan, Y., Wcisło, P., Finenko, A. A., Nelson, K., Bernath, P. F., Birk, M., Boudon, V., Campargue, A., Chance, K. V., Coustenis, A., Drouin, B. J., Flaud, J. –M., Gamache, R. R., Hodges, J. T., Jacquemart, D., Mlawer, E. J., Nikitin, A. V., Perevalov, V. I., Rotger, M., Tennyson, J., Toon, G. C., Tran, H., Tyuterev, V. G., Adkins, E. M., Baker, A.,

https://doi.org/10.5194/egusphere-2026-4424
Preprint. Discussion started: 14 August 2026

Barbe, A., Canè, E., Császár, A. G., Dudaryonok, A., Egorov, O., Fleisher, A. J., Fleurbaey, H., Foltynowicz, A., Furtenbacher, T., Harrison, J. J., Hartmann, J. –M., Horneman, V. –M., Huang, X., Karman, T., Karns, J., Kassi, S., Kleiner, I., Kofman, V., Kwabia–Tchana, F., Lavrentieva, N. N., Lee, T. J., Long, D. A., Lukashevskaya, A. A., Lyulin, O. M., Makhnev, V. Yu., Matt, W., Massie, S. T., Melosso, M., Mikhailenko, S. N., Mondelain, D., Müller, H. S. P., Naumenko, O. V., Perrin, A., Polyansky, O. L., Raddaoui, E., Raston, P. L., Reed, Z. D., Rey, M., Richard, C., Tóbiás, R., Sadiek, I., Schwenke, D. W., Starikova, E., Sung, K., Tamassia, F., Tashkun, S. A., Vander Auwera, J., Vasilenko, I. A., Vigasin, A. A., Villanueva, G. L., Vispoel, B., Wagner, G., Yachmenev, A., and Yurchenko, S. N.: The HITRAN2020 molecular spectroscopic database, J. Quant. Spectrosc. Radiat. Transf., 277, 107949, https://doi.org/10.1016/j.jqsrt.2021.107949, 2022.

Griessbach, S., Hoffmann, L., Spang, R., and Riese, M.: Volcanic ash detection with infrared limb sounding: MIPAS observations and radiative transfer simulations, Atmos. Meas. Tech., 7, 1487–1507, https://doi.org/10.5194/amt-7-1487-2014, 2014.

Hofmann, D. J. and Solomon, S.: Ozone destruction through heterogeneous chemistry following the eruption of El Chichón, J. Geophys. Res. Atmos., 94, 5029–5041, https://doi.org/10.1029/JD094iD04p05029, 1989.

Khaykin, S. M., de Laat, A. T. J., Godin-Beekmann, S., Hauchecorne, A., and Ratynski, M.: Unexpected self-lofting and dynamical confinement of volcanic plumes: the Raikoke 2019 case, Sci. Rep., 12, 22409, https://doi.org/10.1038/s41598-022-27021-0, 2022.

Klüser, L., Erbertseder, T., and Meyer-Arnek, J.: Observation of volcanic ash from Puyehue–Cordón Caulle with IASI, Atmos. Meas. Tech., 6, 35–46, https://doi.org/10.5194/amt-6-35-2013, 2013.

Kremser, S., Thomason, L. W., von Hobe, M., Hermann, M., Deshler, T., Timmreck, C., Toohey, M., Stenke, A., Schwarz, J. P., Weigel, R., Fueglistaler, S., Prata, F. J., Vernier, J.-P., Schlager, H., Barnes, J. E., Antuña-Marrero, J.-C., Fairlie, D., Palm, M., Mahieu, E., Notholt, J., Rex, M., Bingen, C., Vanhellemont, F., Bourassa, A., Plane, J. M. C., Klocke, D., Carn, S. A., Clarisse, L., Trickl, T., Neely, R., James, A. D., Rieger, L., Wilson, J. C., and Meland, B.: Stratospheric aerosol—Observations, processes, and impact on climate, Rev. Geophys., 54, 278–335, https://doi.org/10.1002/2015RG000511, 2016.

Lacis, A., Hansen, J., and Sato, M.: Climate forcing by stratospheric aerosols, Geophys. Res. Lett., 19, 1607–1610, https://doi.org/10.1029/92GL01620, 1992.

Lecours, M. J., Bernath, P. F., Sorensen, J. J., Boone, C. D., Johnson, R. M., and LaBelle, K.: Atlas of ACE spectra of clouds and aerosols, J. Quant. Spectrosc. Radiat. Transf., 292, 108361, https://doi.org/10.1016/j.jqsrt.2022.108361, 2022.

Lecours, M., Boone, C. and Bernath, P. ACE ash-sulfate aerosol data [Dataset]. Zenodo. http://doi.org./10.5281/zenodo.21479502, 2026

Lund Myhre, C. E., Christensen, D. H., Nicolaisen, F. M., and Nielsen, C. J.: Spectroscopic Study of Aqueous H2SO4 at Different Temperatures and Compositions: Variations in Dissociation and Optical Properties, J. Phys. Chem. A, 107, 1979–1991, https://doi.org/10.1021/jp026576n, 2003.

Maes, K., Vandenbussche, S., Klüser, L., Kumps, N., and De Mazière, M.: Vertical Profiling of Volcanic Ash from the 2011 Puyehue Cordón Caulle Eruption Using IASI, Remote Sens., 8, 103, https://doi.org/10.3390/rs8020103, 2016.

McCormick, M. P., Thomason, L. W., and Trepte, C. R.: Atmospheric effects of the Mt Pinatubo eruption, Nature, 373, 399–404, https://doi.org/10.1038/373399a0, 1995.

https://doi.org/10.5194/egusphere-2026-4424
Preprint. Discussion started: 14 August 2026

Mishchenko, M. I. and Travis, L. D.: Capabilities and limitations of a current FORTRAN implementation of the T-matrix method for randomly oriented, rotationally symmetric scatterers, J. Quant. Spectrosc. Radiat. Transf., 60, 309–324, https://doi.org/10.1016/S0022-4073(98)00008-9, 1998.

Niemeier, U., Timmreck, C., Graf, H.-F., Kinne, S., Rast, S., and Self, S.: Initial fate of fine ash and sulfur from large volcanic eruptions, Atmos. Chem. Phys., 9, 9043–9057, https://doi.org/10.5194/acp-9-9043-2009, 2009.

Peter, T. and Grooß, J.-U.: Polar Stratospheric Clouds and Sulfate Aerosol Particles: Microphysics, Denitrification and Heterogeneous Chemistry, https://doi.org/10.1039/9781849733182-00108, 2011.

Prahl, S.: miepython: A Python library for Mie scattering calculations, , https://doi.org/10.5281/zenodo.7949263, 2026.

Solomon, S.: Stratospheric ozone depletion: A review of concepts and history, Rev. Geophys., 37, 275–316, https://doi.org/10.1029/1999RG900008, 1999.

Vernier, J.-P., Fairlie, T. D., Deshler, T., Natarajan, M., Knepp, T., Foster, K., Wienhold, F. G., Bedka, K. M., Thomason, L., and Trepte, C.: In situ and space-based observations of the Kelud volcanic plume: The persistence of ash in the lower stratosphere, J. Geophys. Res. Atmos., 121, 11,104-11,118, https://doi.org/10.1002/2016JD025344, 2016.

Zhu, Y., Toon, O. B., Jensen, E. J., Bardeen, C. G., Mills, M. J., Tolbert, M. A., Yu, P., and Woods, S.: Persisting volcanic ash particles impact stratospheric SO2 lifetime and aerosol optical properties, Nat. Commun., 11, 4526, https://doi.org/10.1038/s41467-020-18352-5, 2020.